Available online at www.sciencedirect.com
ScienceDirect
Ceramics International 36 (2010) 855–862
CERAMICS INTERNATIONAL
www.elsevier.com/locate/ceramint

Full transition from metal to ceramic by direct oxidation of metallic cobalt powder

Renaud Metz [a,b,*], Jonathan Morel [b,**], Henri Delalu [b], S. Ananthakumar [c], Mehrdad Hassanzadeh [d]

[a] Institut Charles Gerhardt Montpellier, UMR 5253 CNRS-UM2-ENSCM-UM1, UMR 5253, Université Montpellier 2 composante Physicochimie des Matériaux Organisés Fonctionnels, CC 1700, Bâtiment 11 - Bureau 319 - 3ème étage, Case courrier 15-03, Place Eugène Bataillon, 34095 Montpellier Cedex 5, France

[b] Laboratoire Hydrazines et Procédés UCBL-CNRS-ISOCHEM (groupe SNPE) UMR 5179, Université de Lyon, UCB Lyon1, bât. Berthollet 3ème étage, 22 avenue Gaston Berger, 69622 Villeurbanne Cedex, France

[c] Materials and Minerals Division, National Institute for Interdisciplinary Science and Technology (CSIR), Trivandrum 695019, Kerala, India

[d] AREVA Transmission & Distribution, Medium Voltage Switchgear Business, DRC, 1340 rue de Pinville, 34965 Montpellier Cedex 2, France

Received 27 March 2009; received in revised form 9 May 2009; accepted 20 September 2009
Available online 4 November 2009

Abstract

The study deals with the direct oxidation kinetics of micronic cobalt metal particles and its simulation for the complete transition from metal to ceramic. The simulation was also experimentally verified. All the three possible interfaces, Co/CoO, CoO/Co_3O_4 and Co_3O_4/O_2 (air), have been taken into consideration for the simulation. The complete oxidation kinetics has been investigated from the thermogravimetric studies under isothermal conditions in the temperatures 973–1173 K. A quantitative interpretation based on the diffusion of Co or oxygen ions through the grown oxide layer has been proposed. The activation energy for the oxidation kinetics calculated from the Arrhenius law was 161 ± 20 kJ mol^{-1}.

Keywords: Cobalt; Cobalt oxide; Kinetics; Direct oxidation

1. Introduction

'Direct Oxidation' of Alloy Powders [DOPA] is a technique becoming popular for the production of bulk ceramics [1–4]. This route is closely related to the reaction sintering or reaction bonding which is actually devoted for the fabrication of a dense covalent ceramics, e.g. reaction-bonded silicon nitride (RBSN) is made from finely divided silicon powders that are formed into a shape and subsequently reacted in nitrogen atmosphere at >1500 K [5]. Recently a new route based on the principle that at high temperatures a liquid alloy, by its nature, is homogeneous and once it is quenched at faster rates resulted in a non-segregated solid powder is demonstrated [6,7]. Such a solid powder can be directly converted to respective oxide if a complete oxidation is successfully achieved.

The mechanism controlling the oxidation of metals is not completely elucidated and still it is the topic of interest [8]. The existing studies and results are hard to exploit because the studies entirely focus on establishing the corrosion phenomena by the growth of thin oxide layers and not deal with complete oxidation [9–11]. Our objective is simply opposite because it concerns the total oxidation of the particles, as quickly as possible. From the literature, it is understood that the majority of the proposed theories evolved from the surface oxidation of a metal plates, foils or nanoscale metal particle clusters (<10 nm). Only a very few models have been developed for the subject of complete oxidation of metal powders [12–15]. Early work by Gulbransen et al. shows that the crystal structure of a metal phase plays an important role in the extent of oxidation. The hexagonal crystal form of cobalt (cold-rolled) has a higher oxidation rate than the cubic form (annealed) at temperatures

* Corresponding author at: Institut Charles Gerhardt Montpellier, UMR 5253 CNRS-UM2-ENSCM-UM1, UMR 5253, Université Montpellier 2 composante Physicochimie des Matériaux Organisés Fonctionnels, CC 1700, Bâtiment 11 - Bureau 319 - 3ème étage, Case courrier 15-03, Place Eugène Bataillon, 34095 Montpellier Cedex 5, France.
** Today address: Tridelta Parafoudres S.A. Boulevard de l'Adour - BP 256, 65202 Bagnères de Bigorre Cedex, France.
E-mail address: Renaud.Metz@univ-montp2.fr (R. Metz).

0272-8842/$36.00
doi:10.1016/j.ceramint.2009.10.010

Nomenclature

ν_G, ν_M and ν_{MO} stoichiometry of gas, metal and oxide
G, M and MO gas, metal particles and oxide particles
r_0, r_M and r_{MO} the initial radius of the cobalt particles, the radius of the cobalt and the radius of partially oxidized cobalt oxide particles
ξ the extent of the reaction
m_M^0 and m_M the initial mass of particles and the mass of particles M at time t
t time
ρ_M and ρ_{MO} the metal and oxide density
Δ the Pilling–Bedworth ratio of a metal oxide
D_G the diffusion coefficient of gas
A_M surface of a spherical metal
C_G the local concentration gradient of G at the limit $r = r_M$
C_G^i, $C_G^e C_G$ for $r = r_M$ and C_G for $r = r_{MO}$
'i' and 'e' the initial conditions ($t = 0$) and the equilibrium conditions,

$$\Phi(\xi) = [\Delta/(\Delta - 1)] - (1 - \xi)^{2/3} - [1/(\Delta - 1)][1 + \xi(\Delta - 1)]^{2/3} = \{[\nu_M/\nu_G][D_G C_G^e]/[2\rho_M r_0^2]\}t$$
$$k_{Co}^0(r_0, T, C_A^e) = k_{Co}^0 = [\nu_M/\nu_G][D_G C_G^e]/[2\rho_M r_0^2],$$

τ time necessary to totally consume the reactant M ($\xi = 1$)
Δ_{CoO}, $\Delta_{Co_3O_4}$ the Pilling and Bedworth ratio for CoO and for Co_3O_4
Δ the composite Pilling and Bedworth ratio for CoO–Co_3O_4
m_{Co}^0, m_{Co} and m'_{Co} the initial mass of cobalt, the mass of cobalt at time t which has been transformed to CoO and the mass of cobalt at time t which has been transformed to Co_3O_4,
$a = 2m'_{Co}M_{O_2}/3M_{Co}$, $b = 1/2m_{Co}M_{O_2}/M_{Co}$
M_{O_2}, M_{Co}, M_{CoO} and $M_{Co_3O_4}$ molecular mass of oxygen, cobalt, CoO, and Co_3O_4
E_r^0 activation energy of the global process of oxidation (J mol^{-1})
A_r^0 attempt frequency of the oxidation reaction (min^{-1})
R the gas constant (J mol^{-1} K^{-1})
T temperature (K)

up to 823 K [16]. Co_3O_4 is stable in atmospheric air below 1164 K. Above this range $Co^{II}[Co^{III}]_2O_4$ is reduced to $Co^{II}O$. By means of inert markers of radioactive Pt, Carter et al. [17] show that Co-metal oxidizes by outward diffusion of cobalt atoms through the oxide. Similarly above 973 K, the rate of oxidation is controlled by the diffusion of cobalt cations through the oxide layer. In fact both CoO and Co_3O_4 oxides have the capability to coexist at 973 K [16–21].

Numerous works have been addressed the oxidation of CoO as polycrystalline and rather single crystal plates of several millimetres thick [22–26]. Beyond the fundamental interest of the topic, there has been recent interest for oxygen production using cobalt oxide from the oxidation/reduction cycles [27]. This recent work is based on the phenomenological equation:

$$X(t) = 1 - \exp(-kt^n),$$

where $X(t)$ is the fraction of Co_3O_4 transformed into CoO at time (t). It suggests that diffusion does not limit the conversion of Co_3O_4 to CoO in the range 1113–1213 K as it was believed in the past.

Our paper deals with the oxidation of pure cobalt powders. Studying the oxidation of Co-metal particle to CoO or Co_3O_4 is of course important and relevant in making cobalt oxide dopants for ceramic industries in general and particularly to varistor industries. Also it is an environmental friendly process. Cobalt oxide doped zinc oxide ceramic blocks are used as varistors for the protection of electric or electronic devices against power surges [28]. In the conventional manufacturing of varistors, oxide additives (Co_3O_4, Bi_2O_3, Sb_2O_3, etc.) are usually directly introduced with the reaction mixtures and the main weakness in this case is the difficulty to achieve good chemical homogeneity [29,30]. We have conceived an idea to introduce respective oxide additives as metal particles and then, or simultaneously, convert the metallic powders into oxides having desired qualities by the complete oxidation that can be used for the manufacturing of varistors ceramics [3]. Use of this new route requires the knowledge of the chemical kinetic laws and oxidation mechanisms and therefore we initiated the present study [31]. Also, anticipation of the new international environmental legislation requests strong R&D efforts in order to conciliate market needs and ecological requirements. The route aiming at the direct oxidation of a metal is attractive since on one hand no by-products are produced and on the other hand oxygen from the atmosphere is always available at free of charge.

Although it might be claimed that the oxidation of metallic cobalt may not be relevant to the oxidation of a complex mixture of oxides, where cation diffusion complicates the issue,

oxidation of Co is the simple first fundamental step in the topic of such complex doped zinc alloy system. Therefore we attempt to study the production of pure cobalt oxide via direct oxidation of cobalt metal.

In the beginning, our goal is to examine the oxidation rates assessment of metallic cobalt by means of microbalance method in order to simulate the kinetic of the reaction and check if the metal oxide conversion is indeed limited by the ionic transport of cobalt in Co_3O_4.

2. Experimental

The powder used for this work is a product of Strem Chemicals of 99.8% purity (lot# 143030-8). The powders were classified by sieving according to NFX 11-504 standards. A sample of known weight is passed through a set of sieves of known mesh sizes: 0, 20, 30, 40, 63, 80, 125, 250 and 500 μm. They are mechanically vibrated for a period of time of 2 min. Agglomerates in the range 63 and 80 μm were associated to an average diameter of 71.5, 80 and 125–102.5 μm and so on.

Specific surface area carried out on such powder give a value of $3 \pm 2\ m^2\ g^{-1}$ for the agglomerates range between 63 and 80 μm (micronic-flowmeters/desorption at 150 °C during half an hour).

The variation of the mass of the sample as a function of temperature was followed by thermogravimetry using a LINSEIS L81 thermobalance. The oxidizing gas has a fugacity of 0.21 bar.

The metallic powder was sieved and the particles in the granulometry $63 < \phi < 80$ μm was taken in a curved silica container of 25 mm length and 20 mm width. The mass of the original metal sample weighed (accuracy up 1/10 of mg) was ~50 mg. These conditions allow the formation of an oxide monolayer on the powder kept in the container. A gas flow with sufficient intensity ($3\ L\ h^{-1}$) was maintained to avoid any diminishment of oxygen level at the reaction interface.

Ceramic powder diffraction patterns were recorded on a Siemens diffractometer using Cu $K_{\alpha 1}$ radiation with a wavelength $\lambda = 0.154$ nm between the diffraction angles $2\theta = 5$–90° with a resolution of 0.02° and a time step of 1 s. For determining the relative amounts of Co_3O_4 and CoO, corundum (Al_2O_3, Aldrich, 99.99%) was used as calibration standard. The integrated intensity of the diffraction peaks obtained for each of the known phases was compared. The samples preparation was strictly identical for the entire specimen. For the maximum accuracy in the quantitative determination, the procedure was applied on the five strongest peaks so that the unintentional preferential orientations of the crystallites could be minimized. ICDD files 043-1004 and 043-1467 were used for CoO and Co_3O_4, respectively. It is worth noticing that the cobalt metal calibration was not possible due to fluorescence phenomena (using a X-ray Excalibur Nova (Mo Kα 1–50 W) on a single aggregate: hexagonal phase, *P*63/*mmc* (194), ICDD File 04-001-3273).

Elemental mapping was performed using a Cameca Camebax electron probe microanalyser (EMPA) with an energy dispersive spectrometer. Mapping was performed for resin mounted specimens. This technique was used to evaluate bismuth and oxygen dispersion thorough the diameter of the particles. The relation between composition and microstructure of the resulting materials was investigated by a combination of EPMA and SEM.

3. Results and discussions

The microscopic images of the cobalt metal particles used in the experiments have been presented in Fig. 1. It clearly shows that particles are agglomerate nearly spherical in shape with an average diameter of 50 μm. Agglomerates are made of grains with an average grain diameter of about 1 μm clustered together into a rounded mass as apparent sintered micronic cobalt metal. Making the assumption of a perfect spherical shape and agglomerates constituted by 1 μm particles, the calculated value of specific surface area is consistent with the experimental measured specific area. The surface texture of the particles is therefore negligible. The experiments were conducted isothermally in the temperatures ranging from 973 to 1173 K. Since the reduction of Co_3O_4 to CoO takes place at 1173 K, the experiments were conducted only up to 1173 K [16]. In order to interpret and quantify the extent of oxidation, we consider the following general heterogeneous chemical reaction:

$$\nu_G G(gas) + \nu_M M(solid) \rightarrow \nu_{MO} MO(solid)$$

We have approximated the metal particles (M) as spheres and homogeneous, isotrope and uniform medium (the work of Chowdhry and Coble [25] shows that the diffusion of oxygen in the grain boundary region is faster than Co diffusion on the lattice of CoO only when the grain size is below 30 μm, *i.e.* below the size studied. Our particle diameter is above this range and therefore we might assume that in our study the grain boundaries do not act as fast diffusion paths and the polycrystalline microstructure acts as a single crystal material). Under the given reaction conditions, the initial radius of the cobalt particles, the radius of the cobalt and partially oxidized cobalt oxide particles are designated as r_0, r_M, r_{MO}, respectively. The extent of the reaction may be defined by the expression:

$$\xi = \frac{m_M^0 - m_M}{m_M^0} \tag{1}$$

where m_M^0 is the initial mass of the particles M (M = metal) with an average radius r_0, m_M is the mass of particles M at the time '*t*' with a radius r_M. Since each mass is linked by the particles radius and the metal density (ρ_M):

$$m_M^0 = \frac{4}{3}\pi r_0^3 \rho_M \quad \text{and} \quad m_M = \frac{4}{3}\pi r_M^3 \rho_M$$

the extent of the reaction becomes,

$$\xi = \frac{1 - r_M^3}{r_0^3} \tag{2}$$

Taking the reaction stoichiometry into account, let us express the disappearance of gas and metal and appearance of

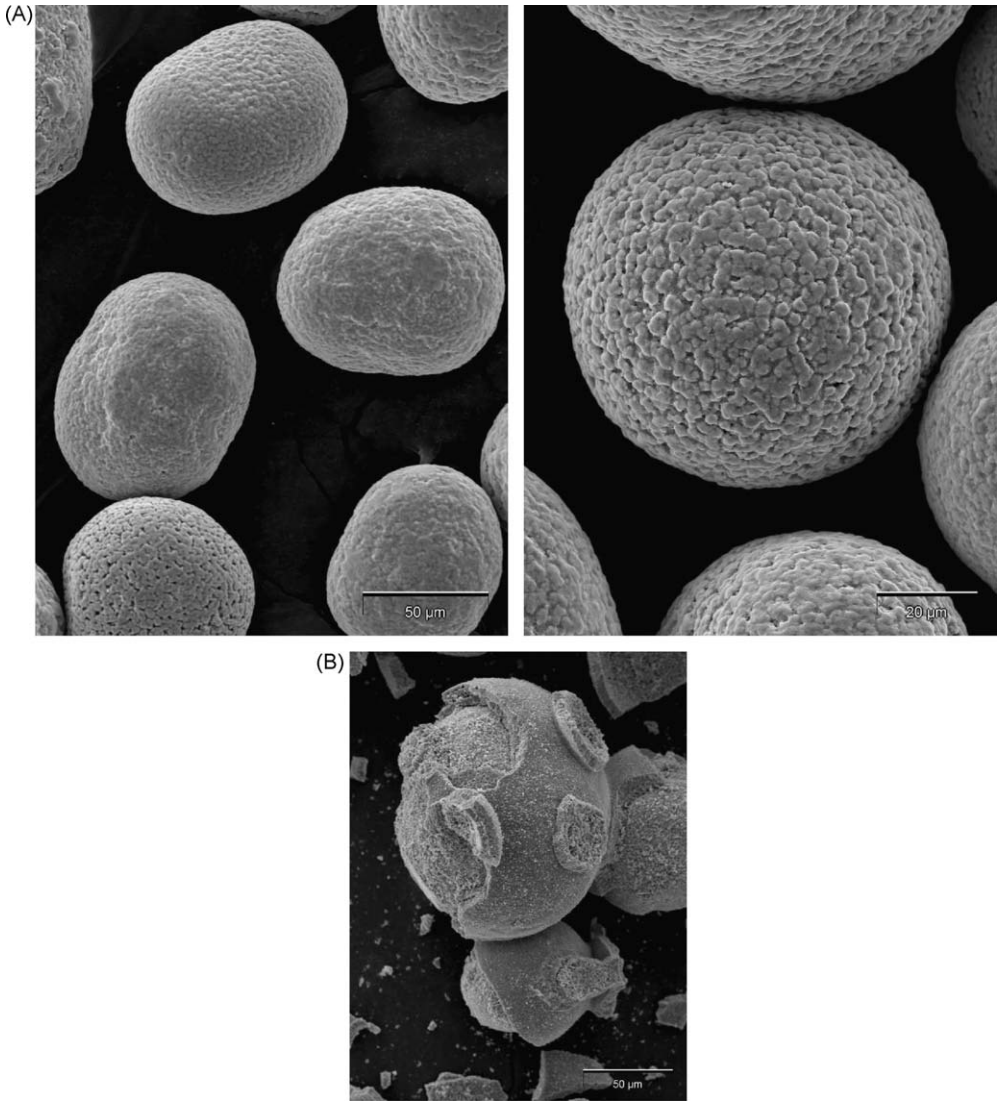

Fig. 1. (A) SEM cobalt particles from Strem Chemicals after sieving: $63 < \phi < 80$ µm. (B) Cobalt particles observed after oxidation (40 wt.%).

oxide species with respect to time (t):

$$-\left[\frac{\mathrm{d}m_{\mathrm{G}}}{\mathrm{d}t}\right] = -\left[\frac{\nu_{\mathrm{G}}}{\nu_{\mathrm{M}}}\right]\left[\frac{\mathrm{d}m_{\mathrm{M}}}{\mathrm{d}t}\right] = +\left[\frac{\nu_{\mathrm{G}}}{\nu_{\mathrm{MO}}}\right]\left[\frac{\mathrm{d}m_{\mathrm{MO}}}{\mathrm{d}t}\right] \tag{3}$$

The Pilling–Bedworth ratio of a metal oxide is defined as the ratio of the volume of the metal oxide that is produced by the reaction between metal and oxygen, to the consumed metal volume [9,13]: $\Delta = V_{\mathrm{MO}}/[V_{\mathrm{M}}^0 - V_{\mathrm{M}}]$.

Hence, the radius of the oxide layer r_{MO}:

$$r_{\mathrm{MO}} = r_0[1 + \xi(\Delta - 1)]^{1/3} \tag{4}$$

Assuming that the diffusion of the reactants through the thickness of the oxide layer is the limiting factor and that the diffusivity of the metal in the oxide lattice is negligible in comparison with the diffusivity of oxygen, application of Fick's law to the gas leads to

$$\frac{\mathrm{d}m_{\mathrm{G}}}{\mathrm{d}t} = -D_{\mathrm{G}}A_{\mathrm{M}}\left\{\frac{\mathrm{d}C_{\mathrm{G}}}{\mathrm{d}r}\right\}_{r=r_{\mathrm{M}}}$$

with $A_{\mathrm{M}} = 4\pi r_{\mathrm{M}}^2$, where D_{G} and $\{\mathrm{d}C_{\mathrm{G}}/\mathrm{d}t\}_{r_{\mathrm{M}}}$ are, respectively the diffusion coefficient and the local concentration gradient of G at the limit $r = r_{\mathrm{M}}$. Substitution of this expression in Eq. (4) reduces to the following rate equation:

$$\frac{\mathrm{d}\xi}{\mathrm{d}t} = \left[\frac{\nu_{\mathrm{M}}}{m_{\mathrm{M}}^0\nu_{\mathrm{g}}}\right]D_{\mathrm{G}}4\pi r_{\mathrm{M}}^2\left\{\frac{\mathrm{d}C_{\mathrm{G}}}{\mathrm{d}r}\right\}_{r=r_{\mathrm{M}}} \tag{5}$$

This relation is integral if r_{M} and the concentration gradient at $r = r_{\mathrm{M}}$ are expressed as functions of ξ. From the lack of accumulation of reactants in the reaction zone (steady-state hypothesis), one can deduce that at a given time 't', the quantity of 'G' which crosses a spherical surface of any thickness is equal to that consumed by the reaction, hence the equality:

$$4\pi r^2 D_{\mathrm{G}}\left\{\frac{\mathrm{d}C_{\mathrm{G}}}{\mathrm{d}r}\right\}_r = 4\pi r^2 DG\left\{\frac{\mathrm{d}C_{\mathrm{G}}}{\mathrm{d}r}\right\}_{r=r_{\mathrm{M}}} \tag{6}$$

Taking into account the limiting conditions ($C_{\mathrm{G}} = C_{\mathrm{G}}^{\mathrm{i}} = 0$ for $r = r_{\mathrm{M}}$ and $C_{\mathrm{G}} = C_{\mathrm{G}}^{\mathrm{e}}$ for $r = r_{\mathrm{MO}}$, where 'i' and 'e' stand, respectively for the initial and equilibrium conditions), one can

write: $\int(C_G^i, C_G^e)dC_G = r_M^2(dC_G/dr)_{r=r_M}\int(r_M, r_{MO})dr/r^2$ from which the expression of the gradient at $r = r_M$ can be linked to ξ via relations (2) and (3):

$$\left\{\frac{dC_G}{dr}\right\}_{r=r_M} = \left[\frac{r_{MO}}{r_M[r_{MO}-r_M]}\right]C_G^e \quad (7)$$

The former expression (7) considers a linear concentration gradient instead of chemical potential differences. (The reality of this assumption depends on the relative ability of the oxide to vary in the stoichiometry which is rather difficult to verify, especially in the presence of grain boundaries which further complicates any description of gradients.)

Substitution of the relation (6) into expression (5) allows us to obtain a differential equation depending only on the variables ξ and t:

$$\frac{d\xi}{dt} = \left[\frac{\nu_M}{\nu_G}\right]\left[\frac{4\pi D_G C_G^e}{m_M^0\{1/[r_0(1-\xi)^{1/3}]-1/[r_0[1+\xi(\Delta-1)]^{1/3}]\}^{-1}}\right]$$

which after integration, leads to the following final equation:

$$\left[\frac{\Delta}{\Delta-1}\right] - (1-\xi)^{2/3} - \left[\frac{1}{\Delta-1}\right][1+\xi(\Delta-1)]^{2/3} = \left[\frac{[\nu_M/\nu_G][D_G C_G^e]}{2\rho_M r_0^2}\right]t$$

$$\Phi(\xi) = k_{Co}^0(r_0, T, C_A^e)t = k_{Co}^0 \quad (8)$$

One can define:

$$k_{Co}^0(r_0, T, C_A^e) = k_{Co}^0 = \left[\frac{[\nu_M/\nu_G][D_G C_G^e]}{2\rho_M r_0^2}\right]$$

k_{Co}^0 which is proportional to the diffusion constant, can be related to the observed rate constant of the reaction. For a fixed value of the particle size, temperature, and composition of gas, the constant k_{Co}^0 is experimentally determined at any time from the parameters (ξ, t). In particular, the time necessary to totally consume the reactant M ($\xi = 1$) is equal to: $\tau = [1/k_{Co}^0][\Delta/(\Delta-1)]\{1-[1+\xi(\Delta-1)]^{2/3}/\Delta\}$.

It is worth noticing that the integrations are carried out assuming that oxygen is adsorbed at the surface of the cobalt metal and is then dissociate before to diffuse through the growing oxide layer: O_2 (gas) $\rightarrow O_{2,ads} \rightarrow O^{2-}$. Since the metal out-diffuses through the growing oxide layer, this mechanism may not hold good [9,10,17,32]. However the present model can be used in both configurations because it cannot identify the nature of the diffusing species. Moreover, it is not possible to establish if the diffusion is limited by the CoO layer (rock salt structure) or the Co_3O_4 layer (spinel structure). An interesting study reported in Ref. [33] attests that there are two cases to be considered depending on whether CoO single crystals are grown and annealed in air or Ar. Oxygen diffusion possibly make clusters formation of Co_3O_4 in CoO which are disassociated by annealing leading to non stoichiometric CoO [33]:

$$CoO(Co/O = 1) + Co_3O_4(Co/O = 3/4) \rightarrow Co_{1-\delta}O(Co/O = 1-\delta = 0.9999 \text{ or } 0.99)$$

On the contrary, single crystals grown and annealed in Ar lead to slower oxidation kinetic and non-parabolic law [33]. The control of the diffusion by outward cobalt migration in Co_3O_4 layer, reported to be always stoichiometric and it is also experimentally confirmed, *e.g.* by inert gold markers [32] is therefore reasonable.

X-ray powder diffraction carried out on the partially oxidized specimens show the presence of two oxides: CoO and Co_3O_4. This is in agreement with the literature where the nanometric and micronic oxide layers observed at the surface of bulk metallic samples are constituted of two oxides [9,10,16]: an inner and outer layer of $Co^{II}O$ and $Co^{II}Co^{III}{}_2O_4$, respectively. The simultaneous presence of two oxides at the surface of the metal particles, with relative amounts of each oxide changing with temperature and time, lead us to consider a composite Pilling and Bedworth ratio:

$$\Delta = \%_{CoO}\Delta_{CoO} + \%_{Co_3O_4}\Delta_{Co_3O_4}$$

where $\%_{CoO}$ and $\%_{Co_3O_4}$ are the respective amount of each oxide calculated from the ratio $m_{Co_3O_4}/m_{CoO}$, Δ_{CoO} and $\Delta_{Co_3O_4}$ being relative to Co/CoO (1, 69) and Co/Co_3O_4 (2) [9].

To take into account the change in the relative amount of each oxide with temperature, we have named:

$m_M^0 = m_{Co}^0$ the initial mass of cobalt,

m_{Co} and m'_{Co} are the fractions of mass m_{Co}^0 resulting from the chemical reactions:

$$Co + (4y+z)/2O_2 \rightarrow (1-3y-z)Co + yCo_3O_4 + zCoO$$

and a and b the oxidation resulting from the respective chemical reactions:

$$3Co + 2O_2 \rightarrow Co_3O_4 \quad a = \frac{4m'_{Co}M_{Mo}}{3M_{Co}} \quad (9)$$

$$Co + (1/2)O_2 \rightarrow CoO \quad b = \frac{m_{Co}M_{Mo}}{M_{Co}} \quad (10)$$

M_{O_2} and M_{Co} being the molecular mass of the oxygen and cobalt, respectively.

Since $m_{CoO} = [M_{CoO}m_{Co}]/M_{Co}$ and $m_{Co_3O_4} = [m'_{Co}/3M_{Co}]M_{Co_3O_4}$ (9) and (10) can be written as:

$$m_{CoO} = \frac{bM_{MO}}{M_{CoO}}$$

$$m_{Co_3O_4} = \left[\frac{a}{4M_O}\right]M_{Co_3O_4}$$

hence

$$\frac{m_{Co_3O_4}}{m_{CoO}} = \left[\frac{a}{4b}\right]\left[\frac{M_{Co_3O_4}}{M_{Co}}\right] \quad (11)$$

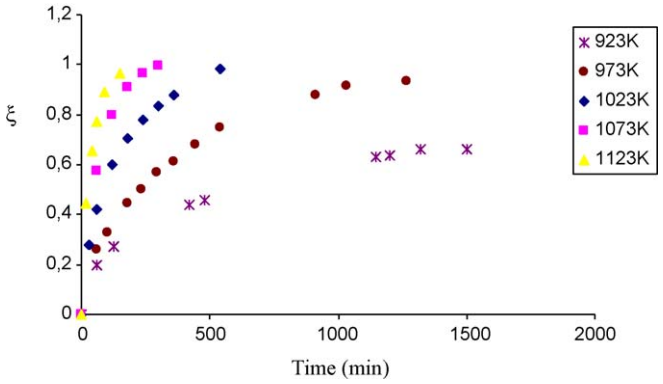

Fig. 2. Extent of the full oxidation of cobalt particles for five isotherms (m_0 = 50.0 mg and particles diameters between 63 and 80 μm).

Quantitative powder X-ray diffraction was carried out on the partially oxidized powder in order to determine the ratio of CoO phase versus Co_3O_4 in each specimen, i.e. the ratio (11). Only the main peaks (100% relative intensity) were considered for each oxide. Taking into account the experimental mass gain $\Delta m = a + b$, it is possible to estimate the true extent of the reaction:

$$\xi = \frac{m^0_{Co} - m^{unoxidized}_{Co}}{m^0_{Co}} \quad \text{since} \quad m^{unoxidized}_{Co} = m^0_{Co} - m_{Co} - m'_{Co}$$

Fig. 2 shows the general trend of the oxidation curve from 923 to 1123 K.

Fig. 3 depicts the plot $\Phi(\xi)$ versus time. It is a line passing through the origin with the slope 'k' and a correlation coefficient better than 0.99. The numeric values of the rate constants are reported in Table 1. In order to check the validity of the model, a series of measurements were carried out by varying the size of the particles from 35 to 187.5 μm. The trials were performed isothermally and the results collected are presented in Table 2 and Figs. 4 and 5.

The slope near to 2 (∼1.64) indicates that the rate constant varies linearly with $1/r_0^2$ which confirms the diffusion of the reactants in the solid phase at a given temperature. Indeed, from

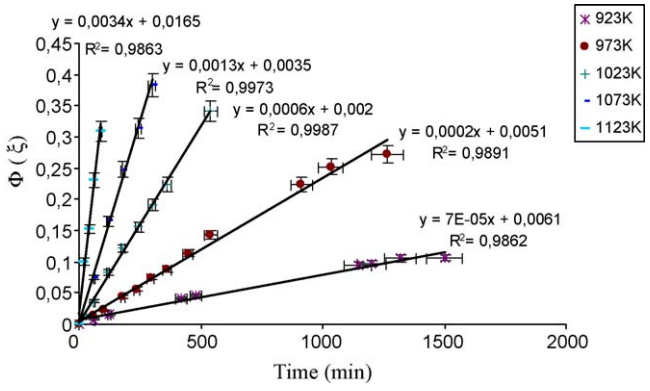

Fig. 3. Rate constant of cobalt oxidation as a function of time (m_0 = 50.0 mg and particles diameters between 63 and 80 μm. R^2 being the correlation coefficient).

Table 1
Rate of oxidation k^0_{Co} versus T and $1/T$.

Temperature (K)	$10^4/T$ (K^{-1})	k^0_{Co} (min^{-1})	$-\ln k^0_{Co}$
923	9.4	0.00008	10.83
973	10.3	0.0002	8.52
1023	9.8	0.0006	7.42
1073	9.3	0.0013	6.65
1123	8.9	0.0034	5.68

Table 2
Influence of agglomerate size on the oxidation rate (T = 973 K).

Average diameter (μm)	Average radius (m)	$\ln r$	k^0_{Co} (min^{-1})	$-\ln k^0_{Co}$
35	17.5E−6	−8.65	0.0007	7.26
71.5	35.7E−6	−7.93	0.0002	8.52
102.5	51.2E−6	−7.57	0.00016	8.74
187.5	93.7E−6	−7.97	0.00004	10.13

(8), the rate of the reaction can be written as:

$$-\ln k^0_{Co} = -\ln\left[\frac{2D_{O_2}C^e_{O_2}}{3\rho_{Co}}\right] + 2\ln r_0$$

Table 2 summaries the k^0_{Co} values obtained for several particles with different grain sizes at 973 K.

Assuming a reaction of the first order, Arrhenius equation gives the dependence of the cobalt oxidation reaction rate

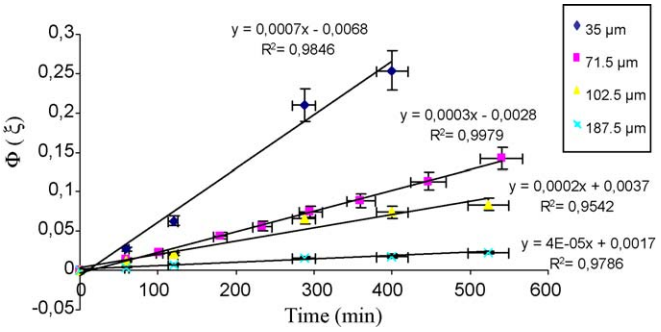

Fig. 4. Plot $\Phi(\xi)$ versus time during the isothermal heating at 973 K – average grain size between 35 and 187.5 μm (m^0_{Co} = 50 mg/R^2 being the correlation coefficient).

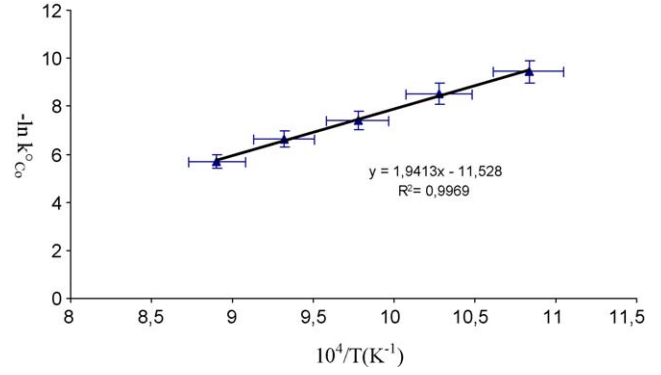

Fig. 5. Arrhenius equation applied to the full oxidation of cobalt particles (R^2 being the correlation coefficient).

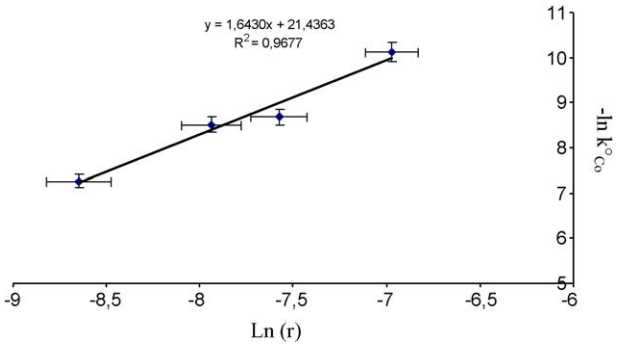

Fig. 6. Validation of the diffusion model for cobalt or oxygen diffusing in the growing oxide layer: evolution of the first order rate constant of the full oxidation of cobalt particles versus the size of the particles (R^2 being the correlation coefficient).

constant at the temperature:

$$k_r^0 = A_r^0 \exp\left[\frac{-E_r^0}{RT}\right] \quad \text{or} \quad -\ln k_r^0 = -\ln A_r^0 + \frac{E_r^0}{RT}$$

where E_r^0: activation energy of the global process of oxidation (J mol^{-1}); A_r^0: attempt frequency of the oxidation reaction min^{-1}; R: the gas constant (J mol^{-1} K^{-1}); T: temperature (K).

The frequency factor and activation energy are extracted from Fig. 6. The numerical values are: $E_{Co}^0 = 1.9413 \times R = 161 \pm 20\,\text{kJ mol}^{-1}$ and $A_{Co}^0 = 101.519 \pm 100\,\text{min}^{-1}$, respectively.

The activation energy value is in good agreement with the value observed from a coarse sample of cobalt of a volume about 1/2 cm^3. We indeed report the activation energy slightly higher compared to 120 kJ mol^{-1} for massive sample. This result might be surprising since one may envisage lower activation energy (a higher constant rate) for the divided matter. However, it is worth to emphasize that the oxidation carried out on the massive sample could not go to completion: after several microns of oxide it was not possible to further oxidize the massive specimen. It is therefore difficult to compare our results with the one obtained from classical parabolic law ([oxide thickness]^2 = 2kt) applied to the growth of the layer on single crystal plates of CoO which lead to the reaction rate constant of about $5 \pm 1 \times 10^{-11}$ cm^2 s^{-1} [18,33–35] to 8×10^{-12} cm^2 s^{-1} [32].

Our results show that the absence of oxygen in the starting material (apparent sintered cobalt metal) lead to a kinetic where the rate is diffusion-controlled. This behavior contrasts sharply with the first per cent of oxidation of sintered pellets of CoO which appeared to be nuclei-growth controlled [22].

A polished cross-section of these metal particles has been examined to assess the powder internal densification. The powder particles were mounted into a polymeric resin and the resin was polished until the particles are cut around the middle. An example of a SEM image is shown in Fig. 7A. The surface

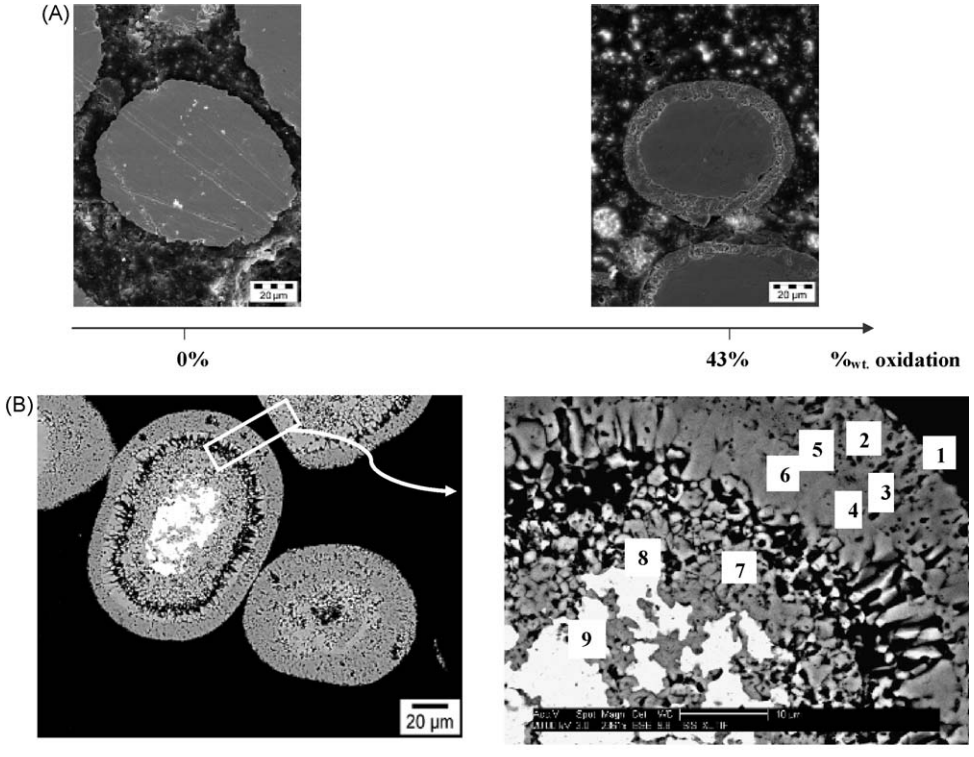

Point	1	2	3	4	5	6	7	8	9
%wt Co	72.9	73.6	75.2	79.3	80.1	81.6	78.6	78.5	99.6
%wt O	27.1	26.4	24.8	20.7	19.9	18.4	21.4	21.5	0.4

Fig. 7. (A) SEM pictures of a cross-section of a cobalt particles and 43 wt.% oxidized (T = 1069 K). (B) Elemental mapping of a cross-section of a cobalt particle oxidized at 90 wt.%. Pictures at different magnifications and point analysis with their location across the diameter of the particle.

of this cross-section presents some scratches due to polishing. It can be noticed that the particle is fully densified and does not show any apparent macroscopic porosity.

After about 40 wt.% of oxidation, the particles present two differentiated area. A metallic core of cobalt and a cobalt oxide ring around it are observed by X-ray mapping relative to oxygen and cobalt (Fig. 7B).

A cross-analysis along the particle diameter shows the profile depicted in Fig. 7B. The center of the particles is composed of pure cobalt. The border of the particle is composed of both cobalt and oxygen. The ratio Co/O agrees with the composition: Co_3O_4. A profile was measured through the diameter of the particle. It appears that the cobalt/oxygen ratio is fairly stable in the oxide layer and decreases drastically at the cobalt–Co_3O_4 interface (points 3 and 4 in Fig. 7B).

4. Conclusion

The study simulates the conditions for the complete oxidation of micronic cobalt powders on the contrary to the earlier studies on the surface oxidation phenomena. We focused on the complete oxidation kinetics of the reactions and found that it is controlled through the diffusion of either cobalt ions or oxygen ions through the grown oxide interface by which the cobalt particles get transformed to oxides. The ceramic formation from the metal particles is achieved by the formation of a duplex microstructure of CoO/Co_3O_4 and diffusion of reactants through it. The reaction follows a first order kinetic with activation energy of 161 ± 20 kJ mol^{-1} between 973 and 1173 K. The study also validates the oxidation kinetics with the respect of the particles size of the cobalt powder.

References

[1] A. Marchand, O. Bucher, H. Delalu, G. Marichy, J.J. Counioux, Fr Patent 91 03550 (1991).
[2] M. Hassanzadeh, C. Machado-Bailly, R. Metz, R. Puyane, EP Patent 1683880 A2 20060726 (2006).
[3] A. Marchand, O. Bucher, H. Delalu, G. Marichy, J.J. Counioux, EP Patent 580912 A1 19940202 (1994).
[4] N. Achard, J.J. Counioux, A. Marchand, G. Marichy, European Journal of Solid State Inorganic Chemistry 34 (1997) 425–451.
[5] http://www.britannica.com (July 8, 2008).
[6] J. Clayton, H. Takamura, R. Metz, H. Tuller, B. Wuensch, Journal of Electroceramics 7 (2) (2001) 113–118.
[7] R. Metz, C. Machado, M. Elkhatib, J.J. Counioux, H. Delalu, K. Al Abdullah, Silicates Industrials 66 (1–2) (2001) 15–23.
[8] P. Schweitzer, Fundamentals of Metallic Corrosion: Atmospheric and Media Corrosion of Metals; Corrosion Engineering Handbook, second edition, CRC Press, 2006.
[9] J. benard, L'oxydation des métaux, processus fondamentaux (I), Gauthier-Villars, 1962.
[10] O. Kubaschewski, B.E. Hopkins, Oxidation of Metals and Alloys, Butterworths and Co., 1962.
[11] R. Tahboud, M. Guindy, H. Merchant, Oxidation of Metals 13 (6) (1979) 545–552.
[12] R. Metz, J. Morel, R. Puyane, M. Hassanzadeh, Journal of the European Ceramic Society 26 (16) (2006) 3741–3752.
[13] R. Metz, R.C. Machado, M. Hassanzadeh, R. Puyane, Journal of Electroceramics 13 (1/2/3) (2004) 825–833.
[14] C. Machado, S. Aidel, M. Elkhatib, H. Delalu, R. Metz, Solid State Ionics 149 (1/2) (2002) 147–152.
[15] R. Metz, C. Machado, M. Hassanzadeh, R. Puyane, Journal of Electroceramics 13 (1/2/3) (2004) 825–832.
[16] E.A. Gulbransen, K.F. Andrew, Journal of the Electrochemical Society 98 (1951) 241–251.
[17] R.E. Carter, F.D. Richardson, C. Wagner, Journal of Metals 7 (1955) 336–343.
[18] H.S. Hsu, G.J. Yurek, Oxidation of Metals 17 (1–2) (1982) 55–76.
[19] S. Mrowec, T. Walec, T. Werber, Corrosion Science 6 (6) (1966) 287–297.
[20] K. Enoki, S. Hagiwara, H. Kaneko, Y. Saito, Nippon Kinzoku Gakkaishi 41 (5) (1977) 505–510.
[21] E.M. Fryt, Oxidation of Metals 12 (2) (1978) 139–156.
[22] W.R. Ott, D.T. Rankin, Journal of the American Ceramic Society 62 (3–4) (1979) 203–205.
[23] A.R. Reti, P.L.T. Brian, L.C. Hoagland, Industrial Engineering Chemistry, Process Designing and Development 5 (2) (1966) 171–177.
[24] S. Mrowec, K. Przybylski, Oxidation of Metals 11 (6) (1977) 383–403.
[25] U. Chowdhry, R.L. Coble, Journal of the American Ceramic Society 65 (7) (1982) 336–342.
[26] J. Nowotny, A. Sadowski, NATO ASI Series, Series B: Physics 129 (1985) 227–242.
[27] K. Hutchings, M. Wilson, P. Larsen, R. Cutler, Solid State Ionics 177 (1–2) (2006) 45–51.
[28] P. Bueno, J.A. Varela, E. Longo, Journal of the European Ceramic Society 28 (2008) 505–512.
[29] R. Puyane, I. Guy, R. Metz, Journal of Sol–Gel Science and Technology 13 (1/2/3) (1998) 575–582.
[30] R. Metz, H. Delalu, J.R. Vignalou, N. Achard, M. Elkhatib, Materials Chemistry and Physics 63 (2000) 157–162.
[31] Y. Sato, T. Yamamoto, Y. Ikuhara, Journal of American Ceramic Society 90 (2) (2007) 242–337.
[32] M. Lafleurielle, F. Millot, G. Dhalenne, A. Revcolevschi, Solid State Ionics 89 (1–2) (1996) 139–145.
[33] J. Païdassi, M.G. Vallée, P. Pépin, Memoires Et Etudes Scientifiques De La Revue De Metallurgie 62 (1965) 857–861.
[34] K. Przybylski, W.W. Smeltzer, Journal of the Electrochemical Society 128 (4) (1981) 897–900.
[35] M.G. Vallée, J. Païdassi, Métaux 42 (1967) 367–372.